The Regulatory Role of NF-κB and Twist1 in Breast Cancer Cells

Bruno R. B. Pires1, Renata Binato[1], Gerson M. Ferreira1, Andre L. Mencalha[2], Stephany Corrêa[1], Barbara Du Rocher[3], Daniel Bulzico[4], Luize G. Lima[5], Carolina Panis[6] and Eliana Abdelhay[1]

[1] Laboratório de Célula-Tronco, Instituto Nacional de Câncer, Rio de Janeiro, RJ, Brazil; [2] Laboratório de Biologia do Câncer, Universidade do Estado do Rio de Janeiro, Rio de Janeiro, RJ, Brazil; [3] Laboratório de Pesquisa sobre o Timo, Instituto Oswaldo Cruz, Fundação Oswaldo Cruz, Rio de Janeiro, RJ, Brazil; [4] Unidade de Endocrinologia Oncológica, Instituto Nacional de Câncer, Rio de Janeiro, RJ, Brazil; [5] Tumour Microenvironment Laboratory, QIMR Berghofer Medical Research Institute, Herston, Queensland, Australia; [6] Laboratório de Mediadores Inflamatórios, Universidade Estadual do Oeste do Paraná, Francisco Beltrão, PR, Brazil.

ABSTRACT

The metastasis of breast cancer (BC) is related to the expression of epithelial-to-mesenchymal transition (EMT)-inducing genes. We sought to examine the role of NF-κB in the regulation of EMT in BC. NF-κB/p65 knockdown resulted in decreased invasiveness and migration, downregulated SLUG, SIP1, TWIST1 and N-CADHERIN transcripts, and upregulated E-CADHERIN transcripts in BC cells. Bioinformatics tools indicated NF-κB binding sites on promoters of EMT genes. Chromatin immunoprecipitation and luciferase reporter assays confirmed this binding on TWIST1, SLUG and SIP1 promoter regions. Thus, NF-κB directly regulates the transcription of EMT-inducing genes in BC. Furthermore, we investigated the role of NF-κB in redox alterations in gene profiles of BC subtypes by microarray assays. The NF-κB knockdown in BC cells led to differential expression of relevant factors involved in glutathione metabolism, cytochrome P450 and cyclooxygenase, suggesting a relationship between the redox balance and NF-κB. Biochemical analyses validated the microarray dataset focused on oxidative stress, which showed a distinct pattern for each of the three studied BC subtype models. We also investigated the role of Twist1, the master regulator of EMT, in BC subtypes. In HER2 patients, TWIST1 was overexpressed. When it was silenced in HER2 BC cells, TWIST1 modified hundreds of genes compared to control cells in microarray assays. In silico analysis revealed correlations between Twist1 and Th17-mediated immune response. IL-17 signaling was examined, and it was observed that TWIST1 knockdown caused the downregulation of leading members of this signaling. In addition, RORγt, the main regulator of Th17 differentiation, was overexpressed in HER2 BC, similar to TWIST1 expression, supporting our hypothesis proposing a link between Twist1 and Th17-like phenotype/IL-17 signaling in HER2 BC. Thus, demonstrated the role of NF-κB in metastatic and redox processes of BC and Twist1 in IL-17 signaling in HER2 BC and a possible relationship between EMT and immune/inflammatory signaling.

RESULTS

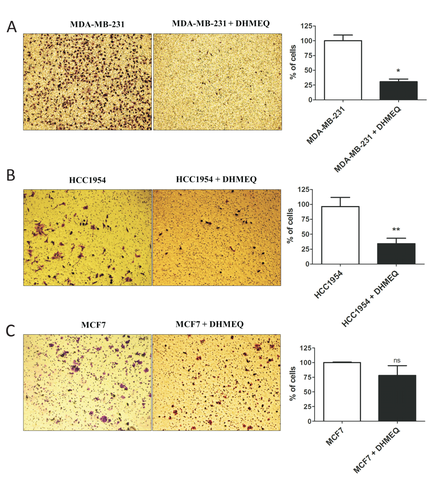

Figure 1. Invasiveness assay. A representative Matrigel transwell assay evaluating invasive potential at 24h after NF-κB/p65 inhibition of MDA-MB-231 (A) HCC-1954 (B) and MCF-7 (C) cells is shown. The bar graph represents the relative invasive potential of MDA-MB-231, HCC-1954 and MCF-7 cells. The cells were stained with crystal violet. Magnification x200. The data were expressed as the mean ± SD. * = p<0.05, ** = p<0.01, ns = not statistically significant.

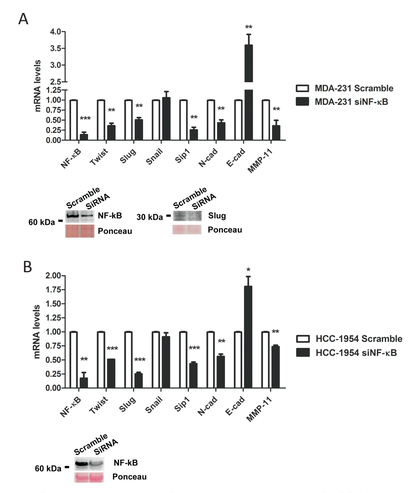

Figure 2. Relative expression of EMT-related genes after NF-κB/p65 genetic silencing using a siRNA approach. The mRNA levels of the EMT-inducing factors SNAIL1, SLUG, TWIST1, and SIP1 and EMT-phenotype markers E-CADHERIN, N-CADHERIN and MMP11 together with NF-κB/p65 inhibition at the protein level were assessed in MDA-MB-231 (A) and HCC-1954 (B) cells (scramble and siNF-κB/p65). Moreover, Slug expression was evaluated at the protein level for MDA-MB-231 by western blot assay in scramble and siNF-κB cells. Ponceau staining was used as a loading control. The data were expressed as the mean ± SD. * = p<0.05, ** = p<0.01, *** = p<0.001.

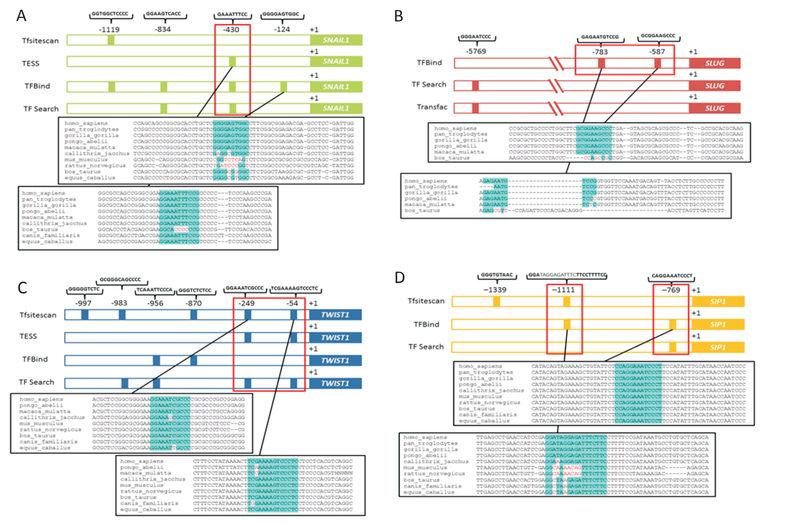

Figure 3. Representative scheme of putative NF-κB binding sites located in the SNAIL1 (A), SLUG (B), TWIST1 (C) and SIP1 (D) promoter regions predicted by Tfsitescan, TESS, TFBind, TFSearch and Transfac bioinformatics tools. An alignment of the DNA region showed evolutionarily conservation among metazoan species. Identical nucleotides are in the blue. Red boxes indicate the regions investigated by chromatin immunoprecipitation. +1: transcription start site.

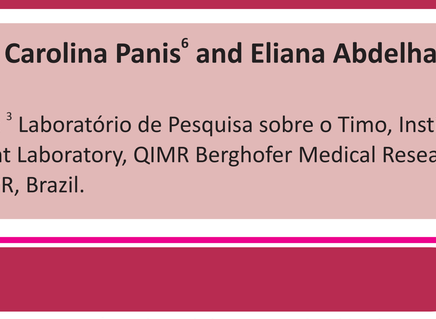

Figura 4. ChIP-qPCR of predicted NF-κB/p65 binding sites in the SNAIL1, SLUG, TWIST1 and SIP1 promoter regions using MDA-MB-231 cells. The histograms set a fold-change of each site by comparing the IgG negative control to NF-κB/p65 antibodies with the natural and NF-κB/p65 inhibited. The data were expressed as the mean ± SD. * = p<0.05, ** = p<0.01, *** = p<0.001.

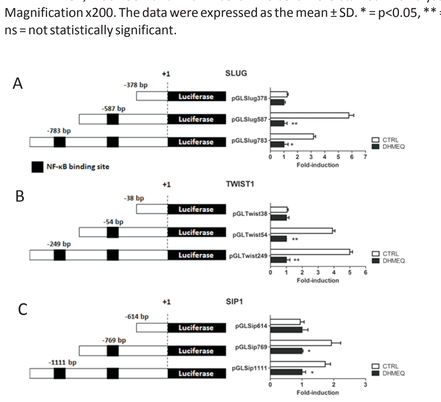

Figure 5. Relative luciferase activity in MDA-MB-231 cells transfected with pGL3-plasmid containing the SLUG (A), TWIST1 (B) and SIP1 (C) promoter regions. The firefly luciferase was normalized to the renilla vector, and the values are relative to the pGL3 (Mock) signal. The black boxes in the schematic plasmid constructs represent NF-κB binding sites. The bar graphs represent the relative luciferase activities of each construct in MDA-MB-231 cells. The white bars indicate natural NF-κB expression, and the black bars show NF-κB inhibition. Each bar represents the mean ± SD.

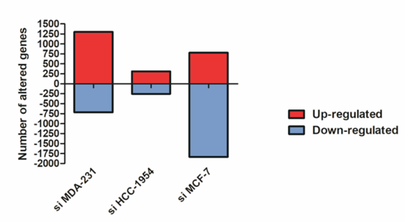

Figure 6. Differentially expressed genes identified by chiparray assay showing increased and decreased genes in breast cancer cells with silenced NF-κB/p65 compared with their scramble counterparts.. Positive values (red columns) correspond to the number of up-regulated genes, and negative values (blue columns) correspond to the number of down-regulated genes.

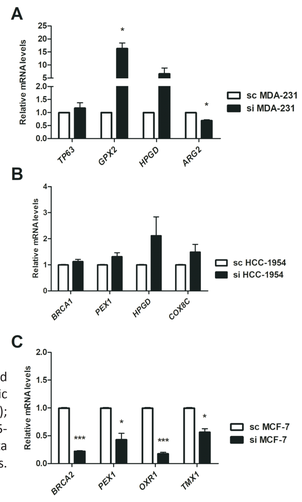

Figure 7. Relative expression qPCR of differentially expressed genes in the microarray analysis after NF-κB/p65 genetic silencing. The mRNA levels were assessed in MDA-MB-231 (A); HCC-1954 (B) and MCF-7 (C) cells, comparing the NF-κB/p65-silenced condition (si) with the Scramble (sc) counterpart. Data are expressed as the means and standard errors of the means. *: p-value < 0.05; **: p < 0.01; ***: p < 0.001.

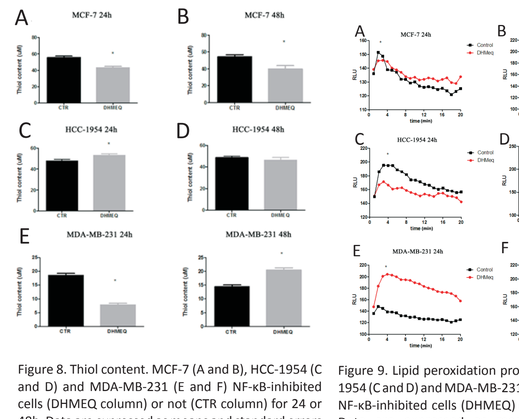

Figure 8. Thiol content. MCF-7 (A and B), HCC-1954 (C and D) and MDA-MB-231 (E and F) NF-κB-inhibited cells (DHMEQ column) or not (CTR column) for 24 or 48h. Data are expressed as means and standard errors of the means. *indicates statistical significance (p<0.05).

Figure 9. Lipid peroxidation profile. MCF-7 (A and B), HCC-1954 (C and D) and MDA-MB-231 (E and F)
NF-κB-inhibited cells (DHMEQ) or not (CTR) for 24 or 48h. Data are expressed as means. *indicates statistical significance (p<0.05).

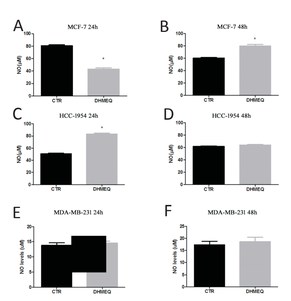

Figure 10. Nitrite as estimative of NO levels. MCF-7 (A and B), HCC-1954 (C and D) and MDA-MB-231 (E and F) NF-κB-inhibited cells (DHMEQ column) or not (CTR column) for 24 or 48h. Data are expressed as means and standard errors of the means. *indicates statistical significance (p<0.05).

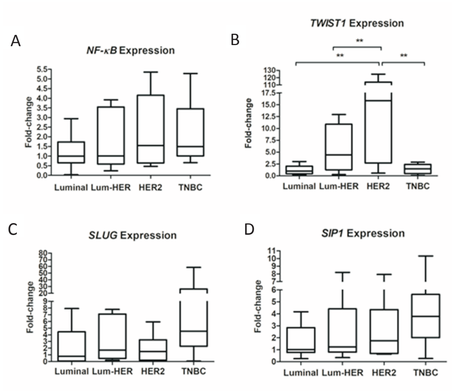

Figure 11. Box-plot graph of NF-κB/p65 (A), TWIST1 (B), SLUG (C) and SIP1 (D) expression in breast cancer subtypes Luminal, Luminal-HER (Lum-HER), HER2 and Triple-negative (TNBC). Median and range of mRNA values are shown. Expression was normalized by ACTB and GAPDH mRNA levels and Ct was calculated vs. Luminal median. Data are shown as the median (± SD). *p<0.05; **p<0.01; ***p<0.001.

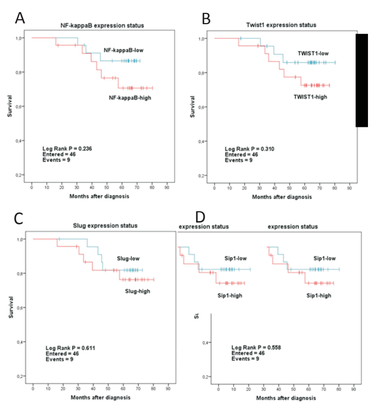

Figure 12. Kaplan-Meier's survival of breast cancer patients stratified according to gene expression of NF-κB/p65 (A), TWIST1 (B), SLUG (C) and SIP1 (D).

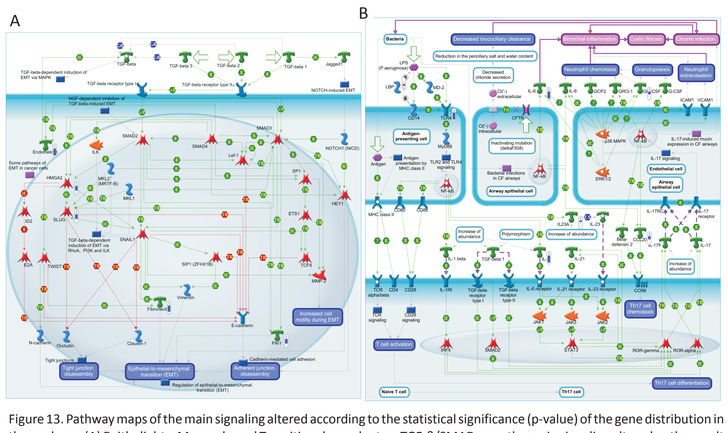

Figure 13. Pathway maps of the main signaling altered according to the statistical significance (p-value) of the gene distribution in the analyzes. (A) Epithelial-to-Mesenchymal Transition dependent on TGF-β/SMADs was the main signaling altered as the result of TWIST1 silencing. (B) Th17-mediated Immune Response was the second signaling more altered in consequence of TWIST1 silencing. The relative gene expression data are visualized on the map by thermometer-like figures in blue (for downregulation) or red (for upregulation).

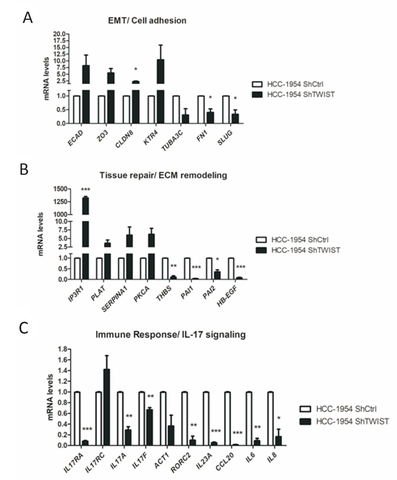

Figure 14. RT-qPCR of the genes altered in the best represented biological processes: (A) Epithelial-mesenchymal transition (EMT)/Cell adhesion, (B) Extracellular matrix (ECM) remodeling/Blood coagulation, and (C) Immune response/IL-17 signaling. ShCTRL = negative silencing control; ShTWIST = TWIST1-knockdown. Data are shown as the mean (± SD). *p<0.05; **p<0.01; ***p<0.001.

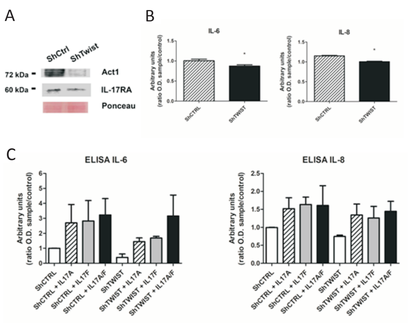

Figure 15. Evaluation of IL-17 signaling in TWIST1-knockdown HER2 breast cancer cells compared with that of control cells. (A) Protein levels of Act1 and IL-17RA in ShCTRL and ShTWIST cells. Staining with Rouge Ponceau was used to ensure that the same sample amounts were loaded for immunoblotting. (B) Levels of secreted IL-6 and IL-8 proteins in the supernatant of ShCTRL and ShTWIST cells. (C) Levels of secreted IL-6 and IL-8 in ShCTRL and ShTWIST cells treated with human recombinant IL-17A, IL-17F or both (IL17A/F). ShCTRL = negative silencing control; ShTWIST = TWIST1-knockdown.

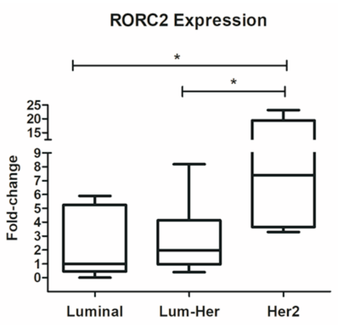

Figure 16. Box-plot graph of RORC2 (RORγt) expression in Luminal, Luminal-Her and HER2 subtypes. Data are shown as the median (± SD). *p<0.05; **p<0.01;

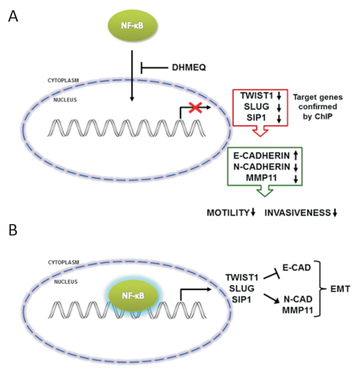

Figure 17. Schematic representation of our main findings. A) Inhibition of NF-κB/p65 translocation reduces the expression of EMT-transcription factors that have been shown to regulate target genes of NF-κB. This inhibition increased E-cadherin expression, decreased N-cadherin and MMP11 expression and reduced cell motility and invasiveness potential. B) Then, NF-κB/p65 transcriptionally regulates the promoter regions of TWIST1, SLUG and SIP1, which in turn represses the epithelial marker E-cadherin and activates the mesenchymal markers N-cadherin and MMP11, resulting in induction of the EMT process. C) Schematic representation of our findings involving Twist1 and IL-17 signaling.

Projeto Gráfico: Área de Edição e Produção de Materiais Técnico-Científicos / INCA